Antitumor and anti-angiogenesis effects of thymoquinone on osteosarcoma through the NF-κB pathway

LEI PENG[1,2*], AN LIU[3*], YUE SHEN[1*], HUA-ZI XU[1], SHI-ZHOU YANG[1,4], XIAO-ZHOU YING[1], WEI LIAO[1], HAI-XIAO LIU[1], ZHONG-QIN LIN[5], QING-YU CHEN[1], SHAO-WEN CHENG[1] and WEI-DONG SHEN[1,3]

[1]Department of Orthopaedic Surgery, The Second Affiliated Hospital of Wenzhou Medical College, Wenzhou, Zhejiang 325000; [2]Department of Trauma Center, The Affiliated Hospital of Hainan Medical College, Haikou, Hainan 570206; [3]Department of Orthopaedic Surgery, The First People's Hospital of Yueyang, Yueyang, Hunan 414000; [4]Zhejiang Cancer Hospital, Hangzhou, Zhejiang 310022; [5]Department of Orthopaedic Surgery, Hospital of Integrated Traditional Chinese and Western Medicine of Wenzhou, Zhejiang 325000, P.R. China

Received July 24, 2012; Accepted October 29, 2012

DOI: 10.3892/or.2012.2165

Abstract. Thymoquinone (TQ), the predominant bioactive constituent derived from the medicinal spice *Nigella sativa* (also known as black cumin), has been applied for medical purposes for more than 2,000 years. Recent studies reported that thymoquinone exhibited inhibitory effects on the cell proliferation of several cancer cell lines. This study was performed to investigate the antitumor and anti-angiogenic effects of thymoquinone on osteosarcoma *in vitro* and *in vivo*. Our results showed that thymoquinone induced a higher percentage of growth inhibition and apoptosis in the human osteosarcoma cell line SaOS-2 compared to that of control, and thymoquinone significantly blocked human umbilical vein endothelial cell (HUVEC) tube formation in a dose-dependent manner. To investigate the possible mechanisms involved in these events, we performed electrophoretic mobility shift assay (EMSA) and western blot analysis, and found that thymoquinone significantly downregulated NF-κB DNA-binding activity, XIAP, survivin and VEGF in SaOS-2 cells. Moreover, the expression of cleaved caspase-3 and Smac were upregulated in SaOS-2 cells after treatment with thymoquinone. In addition to these *in vitro* results, we also found that thymoquinone inhibits tumor angiogenesis and tumor growth through suppressing NF-κB and its regulated molecules. Collectively, our results demonstrate that thymoquinone effectively inhibits tumor growth and angiogenesis both *in vitro* and *in vivo*. Moreover, inhibition of NF-κB and downstream effector molecules is a possible underlying mechanism of the antitumor and anti-angiogenic activity of thymoquinone in osteosarcoma.

Correspondence to: Professor Wei-Dong Shen, Department of Orthopaedic Surgery, The First People's Hospital of Yueyang, 39 Dongmaoling Road, Yueyang, Hunan 414000, P.R. China
E-mail: yyshenweidong@163.com

*Contributed equally

Key words: osteosarcoma, thymoquinone, NF-κB, antitumor, anti-angiogenesis

Introduction

Osteosarcoma is a primary malignant tumor of the skeleton characterized by the direct formation of immature bone or osteoid tissue by the tumor cells. It is an extremely aggressive malignancy that arises mostly in the long bones (1). Limited improvements have been made by using conventional methods including surgery, radiotherapy and chemotherapy in the past two decades (2). Despite the availability of a myriad of treatment modalities, including preferred cytotoxic chemotherapy, dose-limiting toxicity to normal tissues and acquisition of acquired resistance fails to transcend into optimal clinical benefit in terms of cure rate in an overwhelming majority of patients (3,4). Therefore, there is a need for novel strategies involving less toxic agents for their potential in improving the prognosis and therapy of patients with osteosarcoma.

Thymoquinone (TQ) is the bioactive compound derived from black seed (*Nigella sativa*) oil. It is an annual herb that grows in countries bordering the Mediterranean region and in Western Asian countries including India, Pakistan, and Afghanistan. In traditional medicine, thymoquinone is known to be the active principle responsible for many of the seed's anti-oxidant and anti-inflammatory effects (5). Numerous studies have shown that the seeds and oil of this plant are characterized by a very low degree of toxicity (6). Regarding cancer, recent studies showed that thymoquinone exerts anti-proliferative and apoptosis-inducing effects on various tumor cells derived from colorectal carcinoma (7), lung carcinoma (8), myeloblastic leukemia (9) and prostate carcinoma (10). Thymoquinone has also been shown to potentiate the anti-tumor activity of gemcitabine and oxaliplatin in pancreatic cancer (11). Mechanistically, thymoquinone has been reported

to induce apoptosis in tumor cells by suppressing NF-κB, Akt activation, and extracellular signal-regulated kinase signaling pathways and to also inhibit tumor angiogenesis (11-14). Although Roepke *et al* reported that thymoquinone showed inhibitory effects on human osteosarcoma cells (15), whether thymoquinone inhibits osteosarcoma *in vivo* and suppresses osteosarcoma growth through tumor angiogenesis prevention remains unclear.

In the present study, we first sought to understand the molecular mechanism of action of thymoquinone in osteosarcoma cells inducing apoptosis and we tested our hypothesis *in vivo* using an orthotropic model of osteosarcoma. Using *in vivo* data, we show, for the first time, that thymoquinone exerts antitumor and anti-angiogenesis activity in osteosarcoma. These results are correlated with the downregulation of NF-κB and its downstream proteins such as X-linked inhibitor of apoptosis (XIAP), survivin and vascular endothelial growth factor (VEGF) in tumor extracts.

Materials and methods

Reagents. Antibodies were obtained from the following commercial sources: antibodies against survivin, XIAP, Smac and β-actin were obtained from Epitomics (Burlingame, CA, USA), and the caspase-3 antibody was from Abcam (Cambridge, MA, USA). Anti-retinoblastoma antibody was from Santa Cruz Biotechnology (Santa Cruz, CA, USA). Thymoquinone was purchased from Sigma (St. Louis, MO, USA) and was dissolved in DMSO to make 20 mmol/l stock solution. The 0.1% DMSO alone was set as the control group.

Cell culture. Human osteosarcoma cell line SaOS-2 was purchased from American Type Culture Collection (ATCC, Rockville, MD, USA). Mouse osteoblastic cell line MC3T3-El was preserved in our laboratory. SaOS-2 and MC3T3-El cells were maintained in modified Eagle's medium containing 10% fetal bovine serum (FBS), 0.5% penicillin-streptomycin, and 1% glutamine at 37˚C with 5% CO_2. Human umbilical vein endothelial cells (HUVECs; obtained from ATCC) were cultured in gelatin-coated plates with M199 medium containing 20% FBS, endothelial cell growth supplement (50 μg/ml, Sigma) and antibiotics, and incubated at 37˚C in 5% CO_2 in air.

Hoechst 33342 staining for apoptotic nuclei. Morphological changes of SaOS-2 cells were observed under a fluorescence microscope (Olympus, Tokyo, Japan) by the Hoechst staining method. SaOS-2 cells were seeded at a density of $2x10^5$ cells per well onto a 12-well plate for 24 h, followed by incubation with vehicle alone (0.1% DMSO) or 80 μmol/l thymoquinone for 24 h. Following treatment, cells were fixed with 3.7% formaldehyde for 15 min, permeabilized with 0.1% Triton X-100 and stained with 5 mg/ml of Hoechst 33258 for another 5 min at 37˚C. The cells were then washed with PBS and observed under a fluorescence microscope.

Cell viability inhibition by thymoquinone. SaOS-2 cells were seeded at a density of $3x10^3$ cells per well in 96-well culture plates. After overnight incubation, the medium was removed and replaced with fresh medium containing different concentrations of thymoquinone (20, 40 and 80 μmol/l). Following a 24-h incubation, cell viability was determined by CCK-8 assay (Dojin Laboratory, Kumamoto, Japan) according to the manufacturer's instructions. Briefly, CCK-8 solution was added to cells in 96-well plates, the cells were then incubated at 37˚C for 60 min, and absorbance was measured at 570 nm using an MRX Revelation 96-well multiscanner (Dynex Technologies, Chantilly, VA, USA). This experiment was repeated three times.

Flow cytometric assessment of apoptosis. The measurement of phosphatidylserine redistribution in a plasma membrane was conducted according to the protocol outlined by the manufacturer of the Annexin V-FITC/PI apoptosis detection kit (Abcam). After exposing the cells to increasing concentrations of thymoquinone (20, 40 and 80 μmol/l) for 24 h at 6-well plates, harvested $1x10^5$ cells were incubated with 5 μl of Annexin V-FITC and 5 μl of PI for 15 min at room temperature in the dark and then analyzed by flow cytometry using the Cell Quest program (Becton-Dickinson, San Jose, CA, USA).

Tube formation assay. The angiogenesis of HUVEC induced by Matrigel was assessed by the modified methods previously described (12). Briefly, Matrigel (Becton-Dickinson) was dissolved at 4˚C overnight, and each well of pre-chilled 48-well plates was coated with 100 μl Matrigel and incubated at 37˚C for 45 min. HUVECs ($2x10^4$ cells) were seeded onto the Matrigel in 250 μl M199 supplemented with 20% FBS and incubated with various concentrations of thymoquinone (40, 80 and 160 nmol/l) at 37˚C for 24 h in a humidified 5% CO_2 atmosphere. Endothelial cell tube formation was photographed and the light micrograph images were stored in a computer. Tubular structures were quantified by manual counting and percent inhibition was expressed using untreated wells as 100%.

Western blot analysis. At the end of this incubation, cells were washed with ice-cold PBS and lysed in NP40 lysis buffer (20 mmol/l Tris-HCl (pH 7.4), 100 mmol/l NaCl, 1% NP40, 0.5% sodium deoxycholate, 5 mmol/l $MgCl_2$, 0.1 mmol/l phenylmethylsulfonyl fluoride, and 10 mg/ml of protease inhibitor mixture). Protein was extracted using Mammalian Protein Extraction Reagent (Pierce Inc., Rockford, IL, USA) and its concentration was determined by BCA (Pierce) assay. Proteins (30 μg) were separated in 10-15% SDS-polyacrylamide gel electrophoresis (SDS-PAGE) and transferred to a polyphorylated difluoride (PVDF) membrane. Membranes were incubated with primary antibody overnight at 4˚C and then with the respective secondary antibodies. Immunoreactive bands were detected by the enhanced chemiluminescence (ECL) kit for western blotting detection with hyper-ECL film. The same membrane was reprobed with the anti-β-actin antibody, which was used as an internal control for protein loading.

Electrophoretic mobility shift assay. Following treatment, the cells were suspended in 400 μl of ice-cold lysis buffer [1 mol/l HEPES (pH 7.9), 1 mol/l KCl, 0.5 mol/l EDTA, 0.1 mol/l EGTA, 0.1 mol/l DTT, 0.1 mol/l PMSF, 2 μg/ml aprotinin, 2 μg/ml leupeptin, and 0.5 mg/ml benzamidine] for 15 min. The cells were allowed to swell on ice for 20 min and then 4.8 μl of 10% Nonidet P-40 was added to every 400 μl cell

suspension, vortexed, and centrifuged for 1 min at 4˚C. The nuclear pellet was resuspended in 30 μl nuclear extraction buffer [2 mol/l HEPES (pH 7.9), 0.4 mol/l NaCl, 1 mol/l EDTA, 0.1 mol/l EGTA, 0.1 mol/l DTT, 0.1 mol/l PMSF, 2 μg/ml aprotinin, 2 μg/ml leupeptin, and 0.5 mg/ml benzamidine] and incubated on ice with intermittent mixing. The tubes were then centrifuged at 10,000 g for 20 min at 4˚C, and the supernatant (nuclear extract) was quantified using the BCA protein assay. Electrophoretic mobility shift assay (EMSA) was performed by incubating 10 μg of nuclear proteins with IRDye™-700 labeled NF-κB oligonucleotide. The incubation mixture included 2 μg of poly(deoxyinosinic-deoxycytidylic acid) in a binding buffer. The DNA-protein complex formed was separated from free oligonucleotide on 8.0% native polyacrylamide gel using buffer containing 50 mmol/l Tris, 200 mmol/l glycine (pH 8.5), and 1 mmol/l EDTA and then visualized by Imager apparatus. Equal protein loading was ensured by immunoblotting 10 μg of nuclear protein with anti-Rb antibody.

Mouse osteosarcoma models and experimental protocol. Male athymic BALB/c nu/nu mice (4-6 weeks old) were obtained from Wenzhou Medical College. All animals were maintained in the standard mouse plexiglass cages in a room maintained at constant temperature and humidity under 12-h light and darkness cycle. The food, water, and bedding for these immunocompromised mice were sterilized and changed at least once weekly.

The spontaneously metastatic mouse model was developed as previously described (16). Briefly, the left tibia was wiped with 70% ethanol and a 27-gauge needle coupled to a Hamilton syringe was inserted through the tibial plateau with the knee flexed, and 1x10^5 SaOS-2 cells, resuspended in 10 μl PBS, were injected into the marrow space of the proximal tibia. As a control, all animals were injected with controled 0.1% DMSO in the contralateral tibia. After 1 week of implantation, mice were randomized into 2 groups (n=6): a) vehicle alone (control); b) thymoquinone (6 mg/kg given daily by intragastric intubation for 15 days) (6). Serial primary tumor volumes were excised and the final tumor volume was measured using the formula: π x $(d/2)^3$, where d is the diameter of the tumor. Mice were sacrificed 5 days after the last treatment. Half of the tumor tissue was formalin fixed and paraffin embedded for immunohistochemistry and routine H&E staining. The other half was snap-frozen in liquid nitrogen and stored at -80˚C. H&E staining confirmed the presence of tumor(s) in each tissue.

Immunohistochemical analysis. Xenograft tissues of all mice from both the control and the treated groups were harvested at the end of the treatment and fixed with formaldehyde. The fixed tissue was sectioned and immunostaining was performed using primary antibodies specific for Ki-67, CD34 and NF-κB with appropriate dilutions and using normal host serum for negative controls, followed by staining with appropriate HRP-conjugated secondary antibodies. Results were expressed as percentage of Ki-67$^+$ cells ± SE per x40 magnification. A total of ten x40 fields were examined and counted from three tumors of each of the treatment groups. Areas of greater vessel density were then examined under higher magnification (x100) and counted. Any distinct area of positive staining for CD34 was counted as a single vessel. Results were expressed as the mean number of vessels ± SE per high-power field (x100). A total of 20 high-power fields were examined and counted from three tumors of each of the treatment groups. The slides were developed in diaminobenzidine and counterstained with a weak solution of haematoxylin solution stain. H&E was carried out on paraffin-embedded tissue sections. The stained slides were dehydrated and mounted in permount and visualized on an Olympus microscope (Olympus, Japan). Images were captured with an attached camera linked to a computer.

Statistical analysis. Three independent experiments were performed, and data are represented as the mean ± SD for the absolute values or percent of controls. SPSS15.0 software was used for statistical analysis. Statistically significant differences between values obtained under different experimental conditions were determined using the 2-tailed unpaired Student's t-test or χ^2 test. $P<0.05$ was considered to indicate statistically significant differences.

Results

Effect of thymoquinone on cell viability. In order to investigate whether thymoquinone exerts anti-viability effects, SaOS-2 cells were treated with increasing concentrations of thymoquinone (20, 40 and 80 μmol/l) for 24 h, and then the viability of the cells was examined by CCK-8 assays. As shown in Fig. 1B, the viability of SaOS-2 cells was decreased dose-dependently in the presence of thymoquinone.

Thymoquinone induces cell morphological changes. To further examine the cytotoxic effects of thymoquinone on SaOS-2 cells, the cells were treated with 40 μmol/l of thymoquinone for 24 h and then observed under fluorescence microscope by Hoechst 33258 staining. Results showed that there was an increase in the number of irregular nuclear, fragmented nucleus, convoluted nucleus and giant nucleus after treatment with thymoquinone (Fig. 1A), suggesting that the DNA fragmentation was occurring in these cells.

Detection of apoptosis with Annexin V. To determine whether the induction of cell death by thymoquinone could be linked to apoptosis in SaOS-2 cells, we used a method that allows one to detect concurrently viable, necrotic, early apoptotic and late apoptotic cells based on distinct double-staining patterns with a combination of FITC-conjugated Annexin V and PI.

Results clearly demonstrated that treatment with thymoquinone (Fig. 1C) for 24 h increased the percentage of early apoptotic cells in a dose-dependent manner (Fig. 1D). These data indicate that thymoquinone exerts cytotoxic effects which may be mediated by apoptosis on SaOS-2 cells.

Thymoquinone inhibits tube formation of HUVECs. Since the final event during angiogenesis is the organization of endothelial cells in a three-dimensional network of tube, we performed a tube formation assay to investigate the effect of thymoquinone on the capillary-like structure formation of HUVECs. Endothelial cells plated on Matrigel align themselves forming cords, and the tube-like structure formation

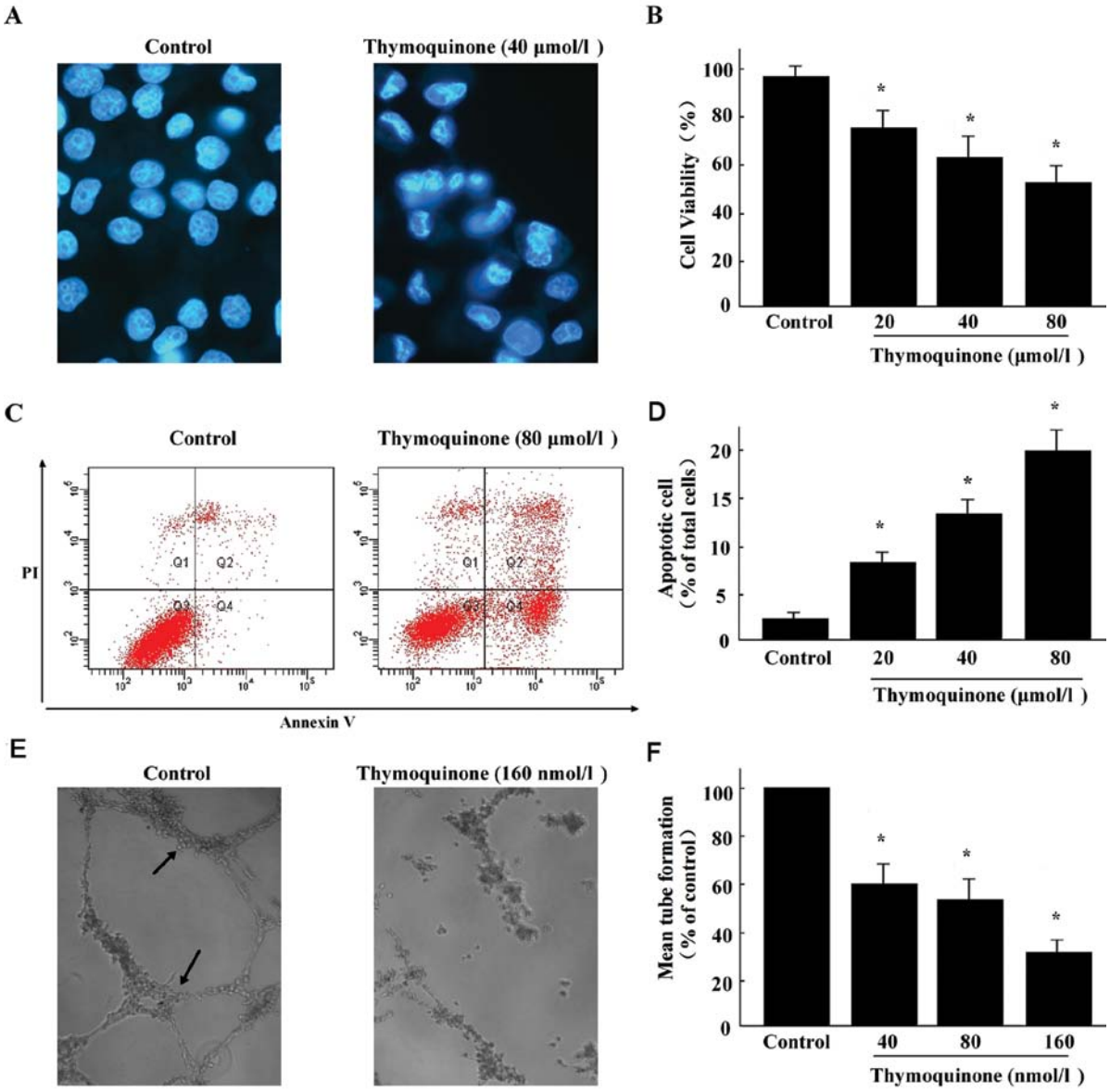

Figure 1. Effect of thymoquinone on cell proliferation, apoptosis and angiogenesis of SaOS-2 cells. (A) SaOS-2 cells were treated with 80 μmol/l thymoquinone for 24 h, nuclei were characterized by Hoechst 33342 assay and investigated under a fluorescent microscope. (B) WST-8 assay showed that thymoquinone inhibited the growth of the SaOS-2 cell line in a dose-dependent manner. (C) SaOS-2 cells were stained with Annexin V and PI and were analyzed by flow cytometry after thymoquinone treatment. Thymoquinone induced apoptosis of SaOS-2 cells in a concentration-dependent manner. (D) Inhibition of endothelial tubule formation on Matrigel by thymoquinone. Data are presented as the mean ± SD of six independent experiments. *P<0.05 vs. control group; **P<0.01 vs. control group.

was maximal within 15 h (Fig. 1E). Treatment of cells with thymoquinone resulted in significant inhibition of tubule formation of HUVECs on Matrigel (Fig. 1F). Our results clearly demonstrate that thymoquinone is effective in controlling the tube formation of endothelial cells *in vitro*.

Thymoquinone inhibits nuclear factor-κB DNA-binding activity. Next, we analyzed whether thymoquinone could abrogate constitutively expressed NF-κB in osteosarcoma cells. SaOS-2 cells were treated with varying doses of thymoquinone (20, 40 and 80 μmol/l) for 24 h and subjected to gel shift assay (EMSA). As shown in Fig. 2A, EMSA revealed that thymoquinone induced a concentration-dependent decrease in NF-κB DNA binding activity in SaOS-2 cells, which was further comfirmed by a supershift experiment. These observations provide strong evidence that thymoquinone is effective in downregulating NF-κB DNA-binding activity.

Thymoquinone inhibits the expression of NF-κB-regulated gene products. We assessed the expression of the NF-κB-regulated genes XIAP and survivin, the overexpression of which has been linked to tumor survival, chemoresistance, and radioresistance, and VEGF, which plays an important role in angiogenesis. Western blotting revealed that thymoquinone induced a concentration-dependent decrease in the levels of these molecules compared with the control treatment in SaOS-2 cells. Western blotting also showed that thymoquinone increased the expression of caspase-3 and Smac (Fig. 2B).

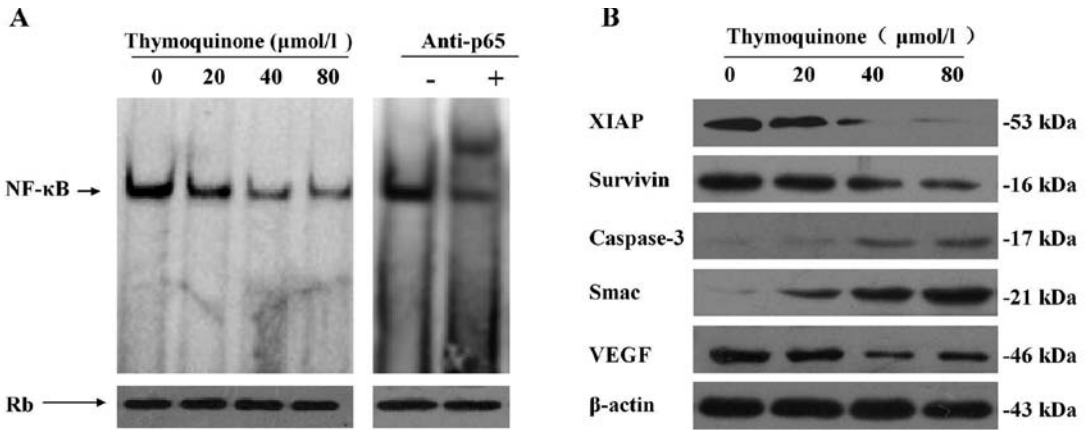

Figure 2. Electrophoretic mobility shift assay (EMSA) and western blot analysis *in vitro*. (A) Gel shift assay showed downregulation of NF-κB in SaOS-2 cells. Equal loading of nuclear protein was ensured by immunoblotting 20 μg of nuclear extract with anti-retinoblastoma antibody by western blot analysis. (B) Western blotting showed alterations in apoptosis-related proteins and VEGF in lysates prepared from SaOS-2 cells following thymoquinone treatment.

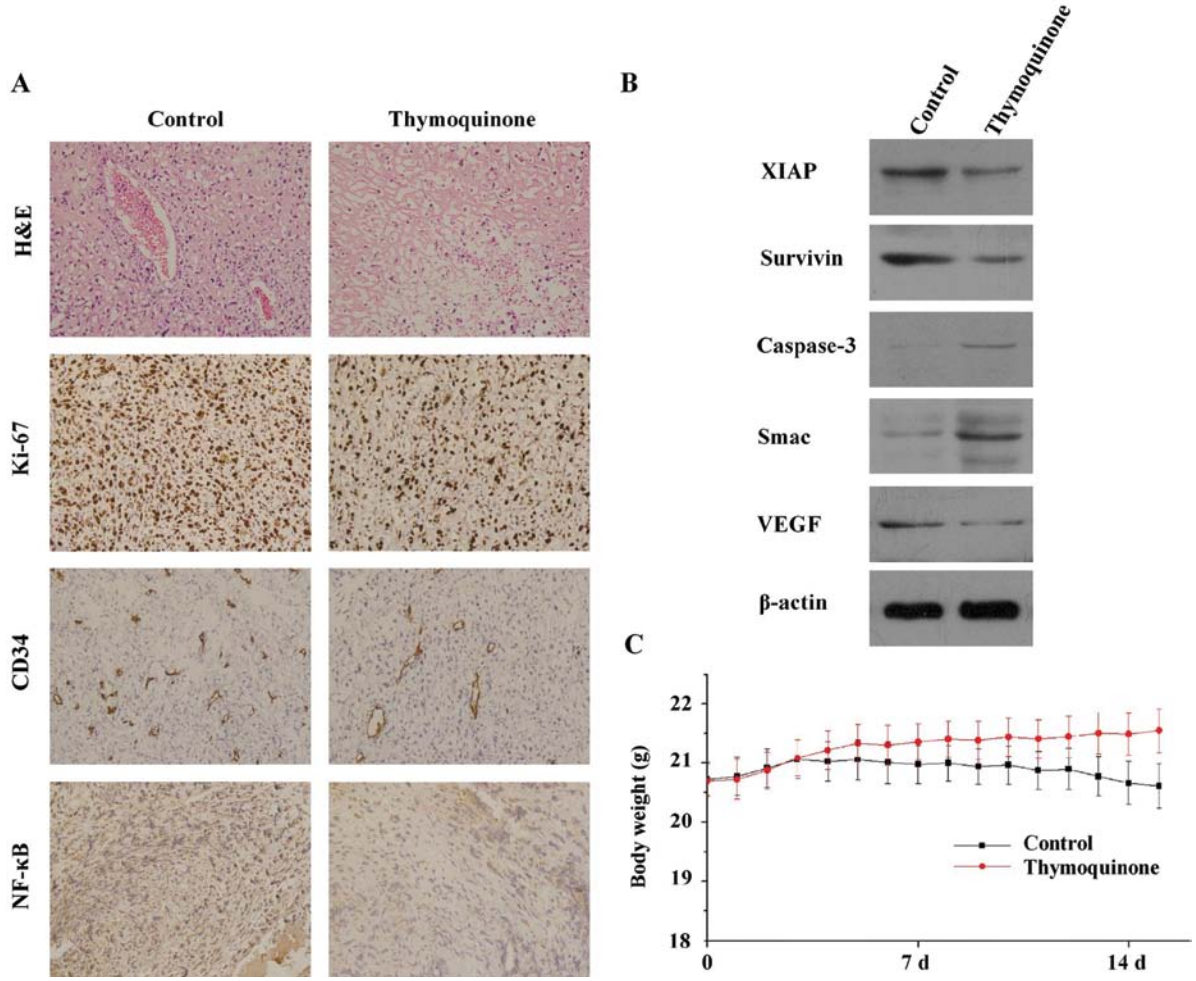

Figure 3. Thymoquinone blocked the growth of osteosarcoma in nude mice. (A) H&E and immunohistochemistry for Ki-67, CD34 and NF-κB in tumor tissue sections (original magnification x200). Immunoreactivity towards all proteins were reduced in the thymoquinone therapy group relative to their expression levels in the untreated control group. (B) Western blotting showed that thymoquinone inhibited the expression of the NF-κB-dependent gene products XIAP, survivin and VEGF in tumor tissues, but the expression of caspase-3 and Smac were upregulated in the thymoquinone-treated group. Samples from three animals in each group were analyzed and representative data are shown. (C) Effects of thymoquinone on mouse body growth.

Thymoquinone inhibits tumor growth in nude mice. For the *in vivo* experiment, 12 mice were divided into two groups as described in Materials and methods. The results showed that after 15 days of treatment with thymoquinone, thymoquinone did not produce significant non-tumor toxicity in tumor-bearing mice. The average mouse body weight of the control group decreased from 22.28±1.22 to 21.24±1.32 g, whereas that of the thymoquinone-treated group increased from 22±1.5

to 24.4±1.2 g (Fig. 3C). The slight decrease of the control group is due to the growth of tumors in the xenograft mice. Next, we determined the mean tumor volume immediately following euthanization in all mice. The mean tumor volume was 74±25 mm^3 in the treated group, vs 126±41 mm^3 in the negative control tumors, resulting in a significant difference of tumor volume in the xenograft model ($P<0.05$).

Tumor histology, immunohistochemistry and protein expression in vivo. H&E evaluation of the tumors from all groups showed high-grade carcinoma associated with tumor apoptosis and necrosis (Fig. 3A). However, there were significant differences in the pattern of necrosis, inflammatory response and fibrosis among the two groups. In the control group, the tumor was largely viable with high mitosis and minimal intratumoral stroma, whereas the peripheral tumor was largely viable and consisted of large nests of neoplastic cells with minimal intratumoral stroma. By contrast, in the group receiving thymoquinone treatment there was marked tumor destruction throughout the entire tumor.

We next examined the expression of the cell proliferation marker Ki-67 and the microvessel density marker CD34 in tumor tissues from the two groups. The results in Fig. 3A showed that thymoquinone significantly downregulated the expression of Ki-67 and CD34 in tumor tissues compared with the control group. For Ki-67, the proliferation index of control was 77.2±5.1%, but the group receiving thymoquinone treatment was 49.3±4.5%. For CD34, the microvessel density was reduced from 192.3±10.2 to 98.6±14.1 after the treatment of thymoquinone. Furthermore, immunohistochemical analysis revealed that the expression of NF-κB was significantly decreased in tumors derived from mice treated with thymoquinone compared with untreated mice. Tumors also revealed downregulation of a few important NF-κB-regulated molecules such as survivin, XIAP and VEGF proteins, which is consistent with our *in vitro* results.

Discussion

Successful treatment with chemotherapeutic agents is largely dependent on their ability to trigger cell death in tumor cells. However, despite rapid advances in diagnostic and operative techniques, osteosarcoma remains one of the most challenging human malignancies to treat, which is partly due to the advanced stage of the disease and the *de novo* chemoresistant behavior to cytotoxic chemotherapeutic agents. Several previous studies demonstrated that certain phytochemicals present in medicinal herbs exert antitumorigenic activity by inducing apoptosis in cancer cells. Thymoquinone has been reported to exert anti-proliferative effects on several cancer cells *in vitro*, which are mediated through the induction of apoptosis (7-11). Thymoquinone also enhanced sensitivity to chemotherapeutic agents in pancreatic and lung cancer (8,11). In this study, we investigated our hypothesis that thymoquinone exerts antitumor effects on human osteosarcoma SaOS-2 cell line proliferation and apoptosis. In agreement with previous studies, we documented that thymoquinone within the range of tested concentrations, is able to directly inhibit cell viability dose-dependently in SaOS-2 cells *in vitro*, and the morphological changes of thymoquinone-treated cells were typical of apoptosis, nuclear condensation, and DNA fragmentation. Furthermore, inhibition of cell growth was correlated with apoptotic cell death. Fluorescence-activated cell sorting (FACS) analysis showed thymoquinone increased the percentages of apoptotic cells in a dose-dependent manner. In agreement with the results of FACS, induced apoptosis by thymoquinone in pancreatic cells was validated by activation of caspase-3 (12). However, the growth of mouse osteoblastic cells did not significantly change by thymoquinone until 80 μmol/l for 24 h. Similar observations have been reported in thymoquinone-treated human pancreatic ductal epithelial cells, suggesting a moderate concentration of thymoquinone does not show cytotoxicity to normal cells. In addition to *in vitro* results, this is the first report to show that thymoquinone is also as an effective antitumor agent in a mouse osteosarcoma model, and significant differences in the percentage of Ki-67-positive cells were noted in tumors derived from the thymoquinone group relative to untreated animals. Our results are consistent with a previous study that no significant variation in body weight was detected in animals after treatment with thymoquinone (12). Taken together, these data suggest that thymoquinone is a potential drug candidate for cancer chemotherapies with low chemotoxic side-effects.

The question remains as to how thymoquinone induces apoptosis in SaOS-2 cells. Emerging evidence has indicated that overexpression of the pro-survival molecules survivin and XIAP, members of the inhibitor of apoptosis protein (IAP) family, are associated with poor prognosis and increased tumor recurrence (17). Recent studies have identified the activation of caspase-3 is blocked by the IAPs (18). However, second mitochondria-derived activator of caspase (Smac) (also known as DIABLO) is released from mitochondria into the cytosol during apoptosis and functions by eliminating inhibitory effects of IAPs on caspase-3 (19,20). Once released from mitochondria upon an apoptotic stimulus, Smac docks to the IAPs via an amino-terminal Reaper motif. This displaces the IAPs from their caspase-binding sites, thereby relieving the block on caspase activation (21). In the present study, we noted that thymoquinone *per se* was effective as a general inducer of apoptosis in SaOS-2 cells by downregulating survivin and XIAP, and upregulating cleaved caspase-3 and Smac. To support our hypothesis, we present evidence documenting a significant reduction of tumors *in vivo* by thymoquinone that was found to be associated with the inhibition of antiapoptotic survivin and XIAP. Thymoquinone was effective in downregulating IAP proteins, survivin and XIAP, not only in osteosarcoma cells *in vitro* but also in preclinical *in vivo* conditions.

Angiogenesis is crucial for the growth of solid tumors not only by supplying oxygen and nutrients for the survival of tumor cells but also by providing the route for metastatic spread. Therefore, angiogenesis has been an attractive target for tumor therapy (22,23). Accumulating evidence has confirmed the expression of VEGF is closely linked with angiogenesis and has validated the theory that inhibition of VEGF is a promising anticancer strategy (24,25). Here, we showed that thymoquinone effectively inhibited human umbilical vein endothelial cell (HUVEC) tube formation. Furthermore, we found that thymoquinone inhibited tumor angiogenesis and prevented osteosarcoma growth in a mouse osteosarcoma model. In agreement with previous studies (12,26), our study

indicates that thymoquinone can effectively suppress angiogenesis both *in vitro* and *in vivo* at this experimental condition. Next we showed that thymoquinone downregulated the expression of VEGF both *in vitro* and *in vivo*, which provided an explanation for its inhibition of angiogenesis observed in the mouse osteosarcoma model.

Extensive studies have demonstrated that the rapid-acting primary transcription factor nuclear factor-κB (NF-κB) is constitutively active in osteosarcoma cell lines (27). Emerging evidence suggests that the DNA-binding ability of NF-κB has been implicated in survivin and XIAP expression and the regulation of apoptosis in various cancer cells (11,25), which underscores the role of NF-κB activation in mediating chemoresistance and that several conventional cancer chemotherapeutic agents activate NF-κB leading to an unfavorable clinical outcome (11,25). Furthermore, tumor angiogenesis is regulated by numerous NF-κB-regulated gene products, including VEGF and TNF (25,28). Finally, evidence indicates the importance of NF-κB in osteosarcoma and suggests that agents that block NF-κB activation could reduce chemoresistance and angiogenesis in osteosarcoma and may possibly be used as a novel therapeutic regimen for osteosarcoma. Previous studies have demonstrated that curcumin (25), genistein (29) and hyperthermia (30) exert antitumor and anti-angiogenesis activity through downregulation of NF-κB. In the present study, we found that thymoquinone abrogates NF-κB activation in osteosarcoma SaOS-2 cells. In addition, our *in vitro* results showed that thymoquinone treatment inhibits NF-κB and exerts anti-proliferative and apoptosis-inducing effects in SaOS-2 cells, suggesting that inhibition of NF-κB by thymoquinone is mechanistically associated with sensitization of osteosarcoma cells to apoptosis. However, most importantly, these *in vitro* results, such as the antitumor activity and inactivation of NF-κB, were recapitulated *in vivo* using the mouse osteosarcoma model, which provides a scientific rationale for the therapeutic exploitation of our strategy for the treatment of patients with osteosarcoma. These results provide strong molecular *in vitro* and *in vivo* evidence supporting our hypothesis that inactivation of the NF-κB signaling pathway by thymoquinone is likely to be an important and novel strategy for the treatment of osteosarcoma.

In conclusion, our present findings are consistent with the hypothesis that thymoquinone could downregulate antiapoptotic and angiogenesis proteins that are regulated by NF-κB, resulting in loss of osteosarcoma cells to survival. Our *in vitro* findings are consistent with the *in vivo* results and provide support for the further development of thymoquinone as an adjunct to conventional chemotherapeutics by targeted inactivation of NF-κB for the treatment of human osteosarcoma, and the initiation of clinical trials.

Acknowledgements

The authors thank all the staff in the Laboratory of Orthopaedic Research Institute and Scientific Research Center of the Second Affiliated Hospital of Wenzhou Medical College. This study was supported by grants from the National Natural Science Foundation of China (31060135/C100302), Project of Science and Technology Department of Zhejiang Province (2010C34006/2010C34G2090013), Project of Health Department in Hainan Province (No.2011-34) and Science-Technology Hall of Hainan Province (GJXM201102).

References

1. DuBois S and Demetri G: Markers of angiogenesis and clinical features in patients with sarcoma. Cancer 109: 813-819, 2007.
2. Lee JA, Kim MS, Kim DH, *et al*: Relative tumor burden predicts metastasis-free survival in pediatric osteosarcoma. Pediatr Blood Cancer 50: 195-200, 2008.
3. Bacci G, Ferrari S, Mercuri M, *et al*: Neoadjuvant chemotherapy for osteosarcoma of the extremities in patients aged 41-60 years - outcome in 34 cases treated with adriamycin, cisplatinum and ifosfamide between 1984 and 1999. Acta Orthop 78: 377-384, 2007.
4. Chou AJ, Merola PR, Wexler LH, *et al*: Treatment of osteosarcoma at first recurrence after contemporary therapy: the Memorial Sloan-Kettering Cancer Center experience. Cancer 104: 2214-2221, 2005.
5. Worthen DR, Ghosheh OA and Crooks PA: The in vitro anti-tumor activity of some crude and purified components of blackseed, Nigella sativa L. Anticancer Res 18: 1527-1532, 1998.
6. Ali BH and Blunden G: Pharmacological and toxicological properties of *Nigella sativa*. Phytother Res 17: 299-305, 2003.
7. Gali-Muhtasib H, Diab-Assaf M, Boltze C, *et al*: Thymoquinone extracted from black seed triggers apoptotic cell death in human colorectal cancer cells via a p53-dependent mechanism. Int J Oncol 25: 857-866, 2004.
8. Jafri SH, Glass J, Shi RH, Zhang SL, Prince M and Kleiner-Hancock H: Thymoquinone and cisplatin as a therapeutic combination in lung cancer: in vitro and in vivo. J Exp Clin Cancer Res 29: 87, 2010.
9. El-Mahdy MA, Zhu QZ, Wang QE, Wani G and Wani AA: Thymoquinone induces apoptosis through activation of caspase-8 and mitochondrial events in p53-null myeloblastic leukemia HL-60 cells. Int J Cancer 117: 409-417, 2005.
10. Kaseb AO, Chinnakannu K, Chen D, *et al*: Androgen receptor- and E2F-1-targeted thymoquinone therapy for hormone-refractory prostate cancer. Cancer Res 67: 7782-7788, 2007.
11. Banerjee S, Kaseb AO, Wang ZW, *et al*: Antitumor activity of gemcitabine and oxaliplatin is augmented by thymoquinone in pancreatic cancer. Cancer Res 69: 5575-5583, 2009.
12. Yi TF, Cho SG, Yi ZF, *et al*: Thymoquinone inhibits tumor angiogenesis and tumor growth through suppressing AKT and extracellular signal-regulated kinase signaling pathways. Mol Cancer Ther 7: 1789-1796, 2008.
13. Sethi G, Ahn KS and Aggarwal BB: Targeting nuclear factor-kappa B activation pathway by thymoquinone: Role in suppression of antiapoptotic gene products and enhancement of apoptosis. Mol Cancer Res 6: 1059-1070, 2008.
14. Chehl N, Chipitsyna G, Gong QK, Yeo CJ and Arafat HA: Anti-inflammatory effects of the *Nigella sativa* seed extract, thymoquinone, in pancreatic cancer cells. HPB 11: 373-381, 2009.
15. Roepke M, Diestel A, Bajbouj K, *et al*: Lack of p53 augments thymoquinone-induced apoptosis and caspase activation in human osteosarcoma cells. Cancer Biol Ther 6: 160-169, 2007.
16. Al-Romaih K, Somers GR, Bayani J, *et al*: Modulation by decitabine of gene expression and growth of osteosarcoma U2OS cells in vitro and in xenografts: identification of apoptotic genes as targets for demethylation. Cancer Cell Int 7: 14, 2007.
17. Srinivasula SM and Ashwell JD: IAPs: what's in a name? Mol Cell 30: 123-135, 2008.
18. Yang YL and Li XM: The IAP family: endogenous caspase inhibitors with multiple biological activities. Cell Res 10: 169-177, 2000.
19. Verhagen AM, Ekert PG, Pakusch M, *et al*: Identification of DIABLO, a mammalian protein that promotes apoptosis by binding to and antagonizing IAP proteins. Cell 102: 43-53, 2000.
20. Du CY, Fang M, Li YC, Li L and Wang XD: Smac, a mitochondrial protein that promotes cytochrome c-dependent caspase activation by eliminating IAP inhibition. Cell 102: 33-42, 2000.
21. Srinivasula SM, Hegde R, Saleh A, *et al*: A conserved XIAP-interaction motif in caspase-9 and Smac/DIABLO regulates caspase activity and apoptosis. Nature 410: 112-116, 2001.
22. Bergers G and Benjamin LE: Tumorigenesis and the angiogenic switch. Nat Rev Cancer 3: 401-410, 2003.

23. Cooney MM, van Heeckeren W, Bhakta S, Ortiz J and Remick SC: Drug insight: vascular disrupting agents and angiogenesis - novel approaches for drug delivery. Nat Clin Pract Oncol 3: 682-692, 2006.
24. Yu HG, Yu LL, Yang YN, *et al*: Increased expression of RelA/nuclear factor-kappa B protein correlates with colorectal tumorigenesis. Oncology 65: 37-45, 2003.
25. Kunnumakkara AB, Guha S, Krishnan S, Diagaradjane P, Gelovani J and Aggarwal BB: Curcumin potentiates antitumor activity of gemcitabine in an orthotopic model of pancreatic cancer through suppression of proliferation, angiogenesis, and inhibition of nuclear factor-kappa B-regulated gene products. Cancer Res 67: 3853-3861, 2007.
26. Erdurmus M, Yagci R, Yilmaz B, *et al*: Inhibitory effects of topical thymoquinone on corneal neovascularization. Cornea 26: 715-719, 2007.
27. Lamoureux F, Picarda G, Rousseau J, *et al*: Therapeutic efficacy of soluble receptor activator of nuclear factor-kappa B-Fc delivered by nonviral gene transfer in a mouse model of osteolytic osteosarcoma. Mol Cancer Ther 7: 3389-3398, 2008.
28. Aggarwal BB: Nuclear factor-kappa-B: the enemy within. Cancer Cell 6: 203-208, 2004.
29. Banerjee S, Zhang YX, Wang ZW, *et al*: In vitro and in vivo molecular evidence of genistein action in augmenting the efficacy of cisplatin in pancreatic cancer. Int J Cancer 120: 906-917, 2007.
30. Adachi S, Kokura S, Okayama T, *et al*: Effect of hyperthermia combined with gemcitabine on apoptotic cell death in cultured human pancreatic cancer cell lines. Int J Hyperthermia 25: 210-219, 2009.